UA9 report for 2015

Executive Summary

This report describes the activity of the UA9 Collaboration during the last 12 months starting from October 2014. Experimental data were collected in the North Area of the SPS, in the SPS itself and, for the first time, in the LHC. The irradiation of a crystal by high-intensity beams was delayed to 2016, because of the overbooking of the HiRadMat facility at CERN.

The investigations in the North Area were devoted to the characterization of new crystals and detectors. The two crystals installed in LHC during the long shut down LS1 could not be tested in advance with beam because of the shut down itself and of consequent schedule constraints. However, two crystals with almost identical characteristics were produced for a later characterization. These two twin crystals were extensively tested in H8 and provided us with predictions on the behavior of the LHC ones. In addition, 12 crystals of LHC-type were characterized for future applications.

The effect of multiple scattering (MS) of high-energy particles travelling in a crystal depends on the orientation of the crystal with respect to the beam and differs from the one expected in an amorphous block of silicon. MS of 400 GeV/c protons in silicon crystals with different lengths was measured for amorphous orientations, far from the main crystallographic planes and axes where channeling effects are excluded. The experimental data were used to correct the values of the RMS angle of MS and to provide more predictive simulations of crystal-assisted collimation.

Scintillation detector pads located symmetrically around the incoming beam were used to record the frequency of inelastic nuclear interactions (INI) produced during bent crystal traversal. This allowed us to estimate the INI probability both in the case of protons travelling along crystalline planes or axes and in the case of protons travelling far from them.

Some time was devoted to test multi crystals producing large deflection angle through a multi-volume-reflection process, to evaluate focusing crystals with trapezoidal shape and to investigate long crystals producing large channeling angles.

A yet unsuccessful attempt was also made to reveal parametric X-ray radiation produced by high-energy particles during crystal traversal using a novel high-sensitivity directional X-ray detector.

CERN-SPSC-2015-039 / SPSC-SR-173
18/10/2015

GEM, Medipix and Cherenkov detector were tested with beam, characterized and calibrated.

In the SPS only 3 runs could be performed, two in the late 2014 and one in 2015, because of schedule constraints. These runs were used to carefully measure the leakage of the halo particles in the high-dispersion regions of the accelerator during crystal-assisted collimation runs in storage mode with 270 GeV proton beams. Halo particles, leaking from the collimation system are related to protons deflected deeply into the secondary collimator but not stopped by it because of the too short amount of material traversed. A new beam loss detector was located in the dispersive area, downstream of the crystal, in a position where most of the protons emerging from the absorber were already lost in the vacuum pipe, whilst most of the protons having had diffractive interactions in the crystals were still surviving. This extended detector layout allowed us to observe a reduction of the off-momentum particle leakage by a factor of 18 when changing the crystal orientation from amorphous to channeling, this reduction being almost a factor of three larger than in our previous observations.

Last August 30th, crystal channeling was observed for the first time in the LHC. Bent crystals could deflect 450 GeV halo particles surrounding the LHC beam into already existing collimation absorbers, demonstrating that the UA9 devices installed in ring 1 during LS1 are fully operational and suitable for further investigations of crystal assisted collimation in LHC.

Cherenkov detectors were extensively tested both at the North Area test beam and in the SPS in view of their characterization for LHC.

Several publications were issued to illustrate the UA9 results:

. Progress on Cherenkov detectors were presented in various conferences (13th Pisa meeting on Advanced Detectors and LHCP 15);

. The LHC goniometer was discussed at IECON15 conference;

. The SPS results on the off-momentum halo leakage were published in Phys. Lett. B 748 (2015) 451-454;

. Measurements on nuclear dechanneling process were presented in Phys. Lett. B 743 (2015) 440-443;

. Data of multi-strip crystals were presented in Pis'ma v ZhETF, vol 101, iss 10, pp 755-760.

. A doctoral thesis has been completed in 2015. Two PhD and two master theses are in progress.

1. Recall of the UA9 findings in 2014

The results described below are extracted from Ref [1].

1. The UA9 Collaboration with the support of the EN/STI group and of the LHC Collimation Team installed all the necessary devices in the LHC, i.e. high accuracy goniometers and crystals, to test crystal-assisted collimation at the highest possible energy.
2. A routine describing crystal-particle interactions was completed and fully integrated into the LHC-collimation simulation code, based on SIXTRACK. Its predictive power was benchmarked using the experimental results collected in H8 relative to several crystals.
3. Simulations of the SPS experiment demonstrated that the leakage of halo particles in the dispersive area is due both to particles having had diffractive interactions in the crystal and to particles emerging from the secondary collimator with a slightly reduced energy due to ionization. As a consequence of this the loss rate measured in the dispersion suppressor of the SPS is only partially reduced when the crystal is oriented in the optimal channeling direction.

2. UA9 tests in the H8 beam line in the SPS North Area

In the last twelve months, UA9 could take data in H8 during 62 days split over 8 runs. UA9 was main user for 44 days and secondary user for 18 days. The actual time was 70 % of the assignment. The list of the activities and of the main results includes several items.

1. Test of the LHC twin crystals. During LS1 we installed two crystals in LHC not previously tested with beam because of schedule constraints. For each of them, a twin crystal was produced from the same silicon ingot for a later characterization in H8. Unexpectedly, the test in H8 revealed that the strip crystal assembly was unstable, whilst the quasi-mosaic assembly was fully satisfactory. Indeed, the bending angle of each crystal assembly was repeatedly measured in H8 with the UA9 telescope and compared to the value measured with interferometric methods at the end of the

production. The bending angle of quasi-mosaic crystal was consistently measured to be of 38 μrad, sufficiently close to the construction value of 44 μrad. The angle of the strip crystal ST76 instead, was very different from the construction value of 51 μrad and was changing with time by large amounts. This fact was interpreted as a relaxation of the crystal frame, for the first time made of titanium to meet the requirements of the LHC goniometer. Titanium was chosen since it is sufficiently light (as aluminium, which is used in the SPS-type holders) while having a reduced secondary electron emission coefficient. A new design of the strip crystal holder has been launched to mitigate such an effect in order to have predictable bending angle in future strip crystal assemblies.

2. Test of crystals for future use in LHC. A second generation of crystals was produced for LHC. They were repeatedly tested in H8 before and after the thermal cycle required for degassing. Ten quasimosaic crystal assemblies were made available. After tests in H8, before and after thermal cycles, four of them were declared as fully satisfactory. Their bending angles, ranging from 50 to 52 μrad, were well inside the specified one of 50 to 55 μrad, with no measurable change during thermal cycles. Six other assemblies, although very stable during thermal cycles, required a slight adjustment of the holder curvature to reach the specified angular range. After that, all of them were accepted as fully adequate to assist crystal collimation in LHC. Two new strip assemblies were also produced, with a titanium frame submitted to a more severe thermal annealing cycle in view of improving the mechanical stability. The tests performed in the last runs are not yet sufficient to qualify them. More tests are planned to check their long-term stability.

3. Inelastic nuclear interaction studies. The probability of inelastic nuclear interactions of high-energy particles in a bent crystal was measured in 2010 [2]. Such a probability varies considerably with the crystal orientation. For 400 GeV protons and 2 mm long silicon crystals the probability is of 0.5 % in amorphous orientation, slightly larger for volume reflection orientation and by a factor of more than three smaller for optimal channeling orientation. This is of a crucial importance for crystal-assisted collimation in large hadron colliders, since it accounts for the reduced off-momentum halo intrinsically produced by the deflected halo during the crystal traversal. The measurements reported in [2] were obtained by subtracting a steady background recorded statistically in long runs without crystal. The new campaign of measurements

in 2015 was aiming at a direct evaluation and subtraction of the background through high-speed scintillation detectors. The extension to other particle species such as lead ions was also foreseen but not yet completed because of planning constraints. Data were also collected for crystal orientation optimal for axial channeling. In these conditions the inelastic nuclear interaction probability was reduced by a factor close to three with respect to the planar channeling orientation. Two master theses are on going on this subject. A publication will be issued soon.

4. Multiple scattering of high-energy protons along "amorphous" orientations. Strip silicon crystals of 1, 2 and 4 mm lengths were used. As the crystals were slightly bent, the deflection of protons channeled in planar or axial modes could be used to find the angular positions of the (110) planes and <111> axis. Then the amorphous angular position of the crystal at the distance 20 mrad from that axis and 3 mrad from that plane was selected for the measurement of multiple scattering. Large statistic for the distributions of proton deflection angles was accumulated in this amorphous crystal orientation. The measurement of proton deflection angles was performed also without the crystal. It allowed determining the angular resolution of the experiment. The distributions were fitted by a Gaussian and the difference of the mean square deflections for these two cases determined the variance of MS of protons in the crystal. The dependence of the mean square deflection angle of MS on the crystal length obtained in the experiment is shown in Fig. 1. The mean square deflection angle is proportional to the crystal length. The theoretical values performed by Gaussian fits of the Moliere distributions are also shown. The experimental RMS angle value of MS is more than 13% larger than the theoretical one from the Moliere theory for 1 mm long silicon crystal.

5. Other crystals. Tests on multi crystals continued in view of producing an optimal device to be tested for crystal-assisted collimation in the SPS. A photo of such an assembly is shown in Fig. 2. Crystals of this type are not yet optimized for our goal. However, the Collaboration considers them quite promising and therefore important to pursue the efforts for their development. Long crystals of the order of the centimeter are becoming again of interest for UA9 in order to produce large deflecting angles with high efficiency. Preliminary tests have started in H8. In particular, a test of a 20mm long crystal with 250 μrad bending angle and a maximal channeling efficiency, as predicted by simulation, was measured (its radius curvature was ten time larger than

the critical radius at 7 TeV). Tests of bent crystals with focusing properties have continued with some success. In Fig. 3 we show one of the focusing assemblies tested and in Fig. 4 the results obtained.

6. Test of new detectors. Tests of detector configurations were parasitically carried out during the crystal tests with the main silicon telescope of the H8 beam line. Most of the activity was concentrated on the calibration of the Cherenkov detector for proton Flux Measurement (CpFM) response to single particles. Several quartz bars in different configurations were tested in order to choose the best ones for the installation in SPS. One of these configurations with two bars is shown in Fig. 5. Each proton impinging on a quartz bar produces 0.6 photoelectron (see Fig. 6), which is rather consistent with the preliminary measurements performed on the Beam Test Facility of LNF-Frascati. Moreover, a time projection chamber with a 30x30 mm^2 GEM amplification stage and a densely pixelated cathodic readout (55 x 55 μm^2) based on MEDIPIX technology has been successfully tested with a proton beam. Being installed about 60m downstream the crystal it allows a fast and on-line detection of the channeled and of the volume reflected beams (see Fig. 7). This opens new perspectives for future fast measurements of coherent interactions in crystals at H8.
7. Parametric radiation. Parametric X radiation (PXR) is produced in a crystal due to the interaction of the charged particle with multiple crystalline planes. It is highly directional and it might be investigated also in view of an online monitoring of the crystal angular position. PXR produced by high-energy, high-Z ions crossing a crystal was never measured. A first attempt to commission a new X-ray detector has been conducted during the spring test beam period with protons, revealing the necessity of a better shielding. This will be realized for the next Pb ion beam run in H8, not yet carried out due to schedule constraints.

3. UA9 tests in the SPS ring

1. Leakage reduction in crystal assisted collimation of the SPS beam [3]. The UA9 devices for crystal-assisted collimation in the SPS are schematically shown in Fig. 8. In our previous experiments, the collimation leakage was measured by the monitor BLM_2 installed in the first high dispersion (HD) area downstream of the collimator-absorber where off-momentum particles produced in the collimation area have the first

possibility to hit the beam pipe. However, a 60 cm long tungsten bar used as a secondary collimator-absorber is insufficient for the full absorption of the halo protons. Protons deflected by a crystal deeply into the absorber but emerging from it with some momentum loss give a large contribution to the beam losses measured by the monitor BLM_2. Thus, the imperfect absorption of halo protons in our collimator-absorber leads to an underestimation of the efficiency achievable with a crystal-assisted collimation system. Tracking simulations of this process with the SixTrack code including the real beam pipe aperture allowed predicting the azimuth of the second high dispersion area as the place where the loss reduction for the crystal channeling orientation is considerably larger than that observed in the position of BLM_2. Extra beam loss monitors, BLM_3, have therefore been installed at this azimuth. The positions of the monitors BLM_2 and BLM_3 are close to the first and the second dispersion maxima, respectively. Additionally, the betatron phase advance between the absorber TAL and the monitor BLM_2 equals approximately 90°. It is very important because protons strongly scattered in the TAL should acquire a maximal betatron deviation from the orbit near BLM_2. Fig. 9 shows the beam loss dependence on the crystal orientation observed in the new position with monitor BLM_3. The beam loss reduction in channeling is considerably larger, R_{BLM3}=18.1, than in the BLM_2 position where it is about 8. The observation of the large reduction of collimation leakage becomes possible because the number of particles deflected by the crystal in channeling regime deeply inside the TAL, but emerging from it, is considerably reduced on the way to BLM_3 by hitting the beam pipe while traversing the first high dispersion region.

2. Test of the LHC-type goniometer. The new generation of goniometers, designed for the test of the crystal collimation in the LHC, differs significantly from the ones used in the past in SPS. In particular, in order to obtain sub-μrad angular resolutions, a piezo-electric material is used to operate the rotational movement. This choice imposes strict requirements on the weight of the crystal with its support, and requires the implementation of a brand new control system. A complete characterization and commissioning of the two LHC goniometers was performed in the laboratory already before their installation in 2012. However the commissioning without beam in LHC showed an important degradation of the performance of the control system due to some unexpected electronic noise that was not present in the laboratory. Therefore two

new goniometer prototypes were built, to allow further tests in the laboratory and in the SPS, where the access to the device is easier while the environmental conditions are similar with respect to LHC. The tests in the laboratory allowed designing a closed-loop controller with a configurable combination of feed-back and feed-forward signals. The installation in SPS was completed during the Winter Technical Stop in 2015 and the device was available for tests during the first run in 2015. Priority was given to the measurements necessary to validate the operation needed for the LHC data taking. In particular the open-loop and the closed-loop controls were tested and compared for the first time in the presence of the beam. Also, simplified software for non-expert operators was deployed and tested by UA9 users. The first measurements showed a perfect response of the goniometer that was operated successfully at different rotational speeds (from 20 μrad/s to 0.5 μrad/s) and with different angular increments (down to 0.5 μrad). Several angular scans were performed and the channeling angle was identified. Different sequences of movements were issued before returning to the identified channeling orientation to confirm the reproducibility of the device. The only complication concerned the identification of the channeling orientation, which was found displaced by 3 mrad with respect to the position computed from survey data. A review of the procedures followed for the alignment and the survey during the installation is ongoing: while in the past the installation of the crystals was performed in the accelerator after the integration of the goniometers in the beam line, the design of the new goniometers imposes to fix the crystal in the goniometer before the installation in the accelerator. Therefore, the actual alignment of the crystal can be perturbed by several situations, including vibration during the transport, non-nominal direction of the beam pipes in the ring or mechanical deformations due to the pumping of vacuum. Further tests involving the goniometers are planned to verify all the functionalities needed for advanced studies in LHC, including for example the possibility to move the crystal linearly towards the beam while steadily maintaining the channeling orientation.

3. Test of the Cherenkov radiation detector (CpFM). The Cherenkov detector installed upstream the secondary absorber in the SPS is built to measure the flux of the deflected halo particles. The CpFM was successfully installed on the SPS in January 2015 (Fig 10), 58 m downstream the crystal. It was tested for the first time in July. After an initial calibration of its front-end electronics, the quartz radiator bar was

swept through the deflected beam in crystal-assisted collimation mode. A first plot of the collected data is given in Fig. 11. It is well interpolated by an Error-function whose derivative is a Gaussian with a sigma of 1.2 +/- 0.2 mm. Since the CpFM sits 58.48 m downstream the crystal we can derive an angular spread of the channeled beam of 21. +/- 2 μrad in good agreement with the critical angle at 270 GeV.

4. Tests in LHC

The first test in LHC was completed on August the 30th during the 2nd LHC MD block. Both the horizontal and the vertical crystals were tested. Channeling was successfully observed for both crystals through the reduction rate registered by the beam loss monitors downstream of the crystals. In both cases, when the crystal was in channeling, the deflected halo was intercepted predominantly by one of the secondary collimators downstream. This was clearly visible from the distribution of the losses in the entire LHC collimation insertion IR7. Scans of that specific secondary collimator could be performed to probe the transverse distribution of the channeled halo. Both crystals were initially aligned to their respective primary collimator. Before the angular scans, they were inserted by 500μm towards the beam centre in order to become the primary halo collimator. The horizontal crystal was inserted at 5.38 σ, while the vertical crystal was inserted at 5.35 σ from the beam centre. For each alignment the linear position was reproduced within 10 μm tolerance.

Horizontal crystal: the optimal orientation for channeling was observed at the yaw angle of 3160 μrad. The optimum was found by minimizing the loss rate at the BLM just downstream of the crystal; correspondingly the losses at the TCSG where the channeled beam is absorbed (B4L7) were at their maximum. Three different angular scans were made and in all of them the channeling orientation was found at the same yaw angle within 5μrad tolerance. Two scans were performed at 0.5 μrad/s rotational speed with the entire set of primary and secondary collimators in the nominal position for injection energy. One scan, performed at 1 μrad/s speed, was obtained after having retracted all the collimators (both the TCPs and the TCSGs) upstream the crystal position (we refer to this condition as the reduced collimation system). The loss rate as a function of the crystal angle is shown in Fig. 12. The loss reduction factor from amorphous to channeling orientation was found to be of about 39. With the reduced collimation system, keeping the crystal in channeling orientation, we performed a scan of the extracted beam with the collimator used as the secondary absorber (B4L7), as shown in Fig. 13. From the loss rate registered by the BLM downstream of the

B4L7 position we could identify the extracted beam dimension, characterized by an RMS size of 436 μm and the deflection angle of the crystal, whose value was of 60.2 μrad (see Fig.14). Note that this value is very close to the bending angle of the twin horizontal crystal measured in H8, after the relaxation of the crystal frame.

Vertical crystal: The measuring procedure was the same as for the horizontal crystal. Channeling orientation was obtained at the yaw angle = 2250 μrad by observing loss reduction at the BLM just downstream the crystal; the channeled beam was intercepted at the following TCSG (D4L7) where the losses increased accordingly. Also in this case differences of few μrad are observed from an alignment run to another. Two angular scan were recorded. Before the first scan, the crystal was aligned to the primary collimator TCP. Then the TCP was retracted by 1 mm and the crystal orientation was varied at 0.3 μrad/s speed. The second scan, instead, was made with the reduced collimation configuration and a rotational speed of 1 μrad/s. The loss rate recorded during such scan is shown Fig.15. A loss reduction factor of ~ 115 was found. The scan of the extracted beam was performed with the TCSG.D4L7 and the results are shown in Fig. 16. By interpolating the data of the scan we could observe that the extracted beam profile had a sigma value of 584 μm, whilst the bending angle was of 53.1 μrad (see Fig. 17).

In an additional run, both the crystals were simultaneously set in channeling orientation with a reduced set of collimators in IR7. Loss maps were collected. Reference loss maps with the standard collimation system were also recorded for comparisons. The evaluation of the multiturn channeling efficiency and the comparison of the loss maps with both the data collected with the standard collimation configuration and with the predictions of computer simulations are in progress.

5. Plans and perspectives

The perspective of the Collaboration for 2016 includes some ambitious milestones.

One of the main goals for the SPS should be the direct measurement of the collimation leakage in the dispersive areas, using fast detectors such as Cherenkov radiators or, if available, *timepix* detectors of the third generation. A longer absorber cannot be used in UA9 because of mechanical constraints. Therefore, a pair of detectors, one located down stream of the secondary absorber and the other at the first dispersion peak, should allow measuring off-momentum halo leakage, disentangling particles emerging from the secondary absorber from

particles having had a diffractive interaction in the crystal. The flux of the latter type should allow precise evaluations of the reduction factor of the halo leakage from amorphous to channeling crystal orientation. Another important goal consists in comparing the performance of multi-strip crystals operating in multi-reflection mode with that of a single strip crystal operating in channeling mode. Finally, we should bring in routine operation the CpFM Cherenkov detector in view of gaining experience for a possible usage in LHC, and test the LHC-like goniometer in order to simulate LHC ramping-mode operation.

In the H8 area, the plan is to test crystals for LHC with ion species. Another goal is to test multi-strip crystals optimized for the multi-reflection mode in the SPS. Studies to evaluate the performance of focusing crystals and of multi-crystal assemblies should be pursued, together with the investigation of large curvature crystals, suited for large angle deflection.

In LHC, the priority is to continue crystal-assisted collimation tests in both horizontal and vertical planes.

In view of these plans, the Collaboration would like to request in 2016: 20 days in H8 with proton microbeams at 450 GeV and 7 days with ion (Ar or Pb) beams and 4 dedicated days (24 h runs in storage mode) in the SPS.

References

[1] UA9 status report for 2014, SPSC-SR-147.

[2] W. Scandale et al., NIM B 268 (2010) 2655-2659.

[3] W. Scandale et al, Phys. Lett. B 748 (2015) 451-454.

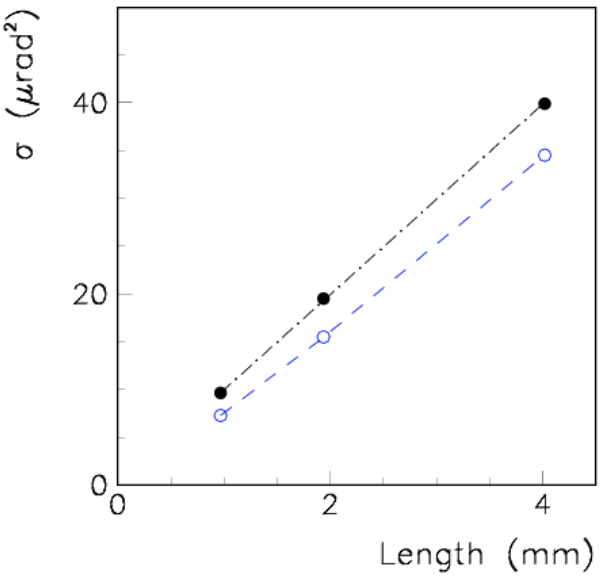

Fig. 1. The dependence of the mean square deflection angle of multiple scattering on the crystal length obtained in the experiment with 400 GeV/c protons (●). The theoretical values performed by Gaussian fits of the Moliere distributions (○).

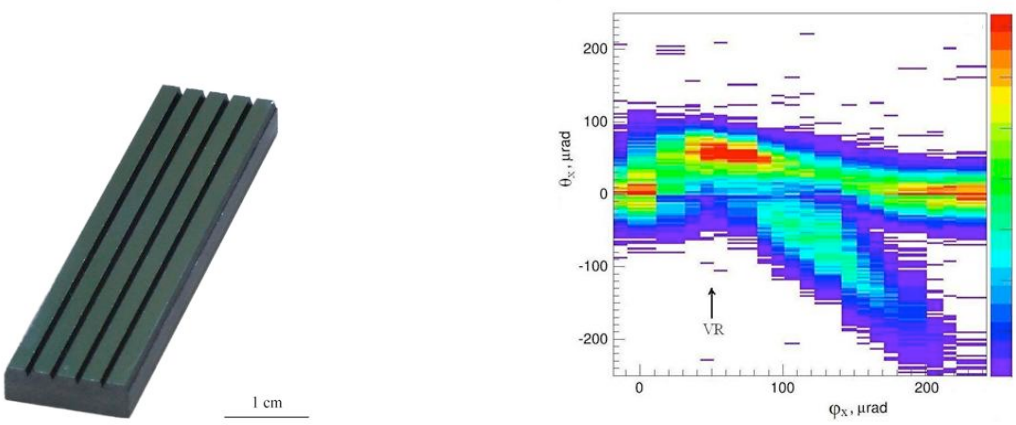

Fig. 2 Photo of the device and 400 GeV/c beam deflection.

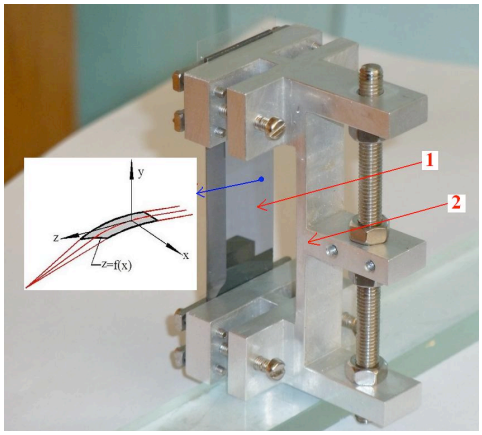

Fig. 3 Photo of focusing crystal device.

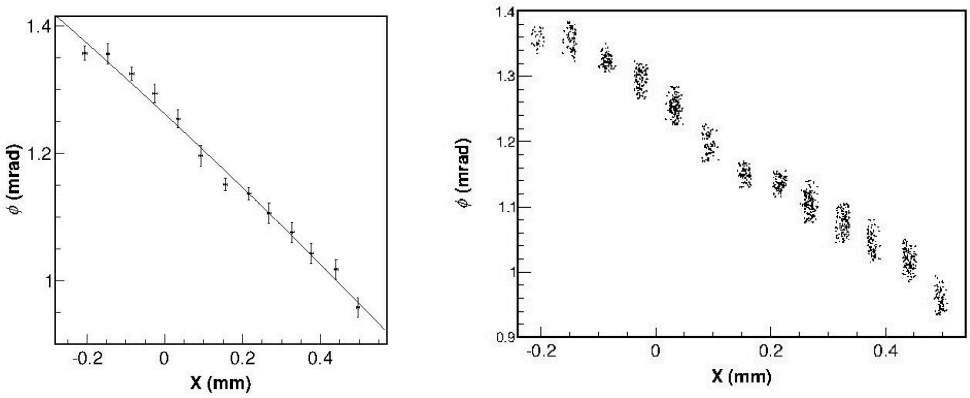

Fig. 4 Linear dependence of bending angle versus transversal coordinate.

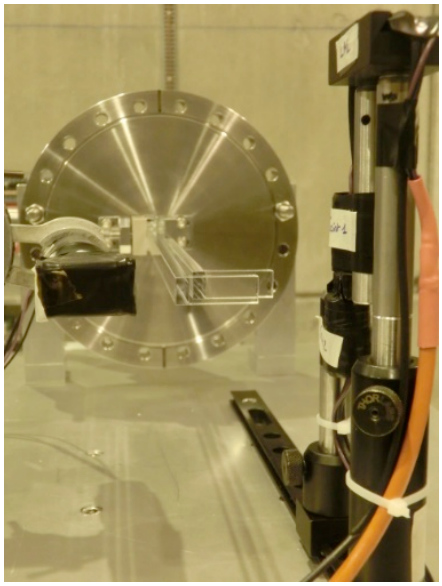

Fig. 5. L-shaped quartz bars tested in H8.

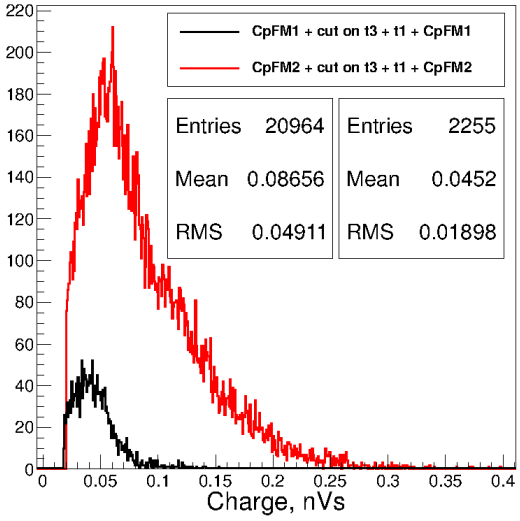

Fig. 6. Charge histogram of the two bars of the CpFM.

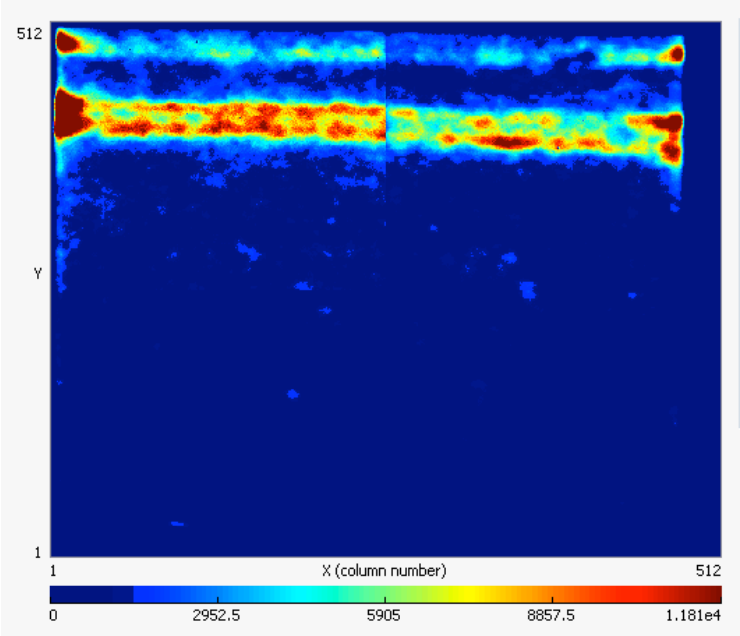

Fig. 7: Online channeled beam monitoring with TPC-GEM

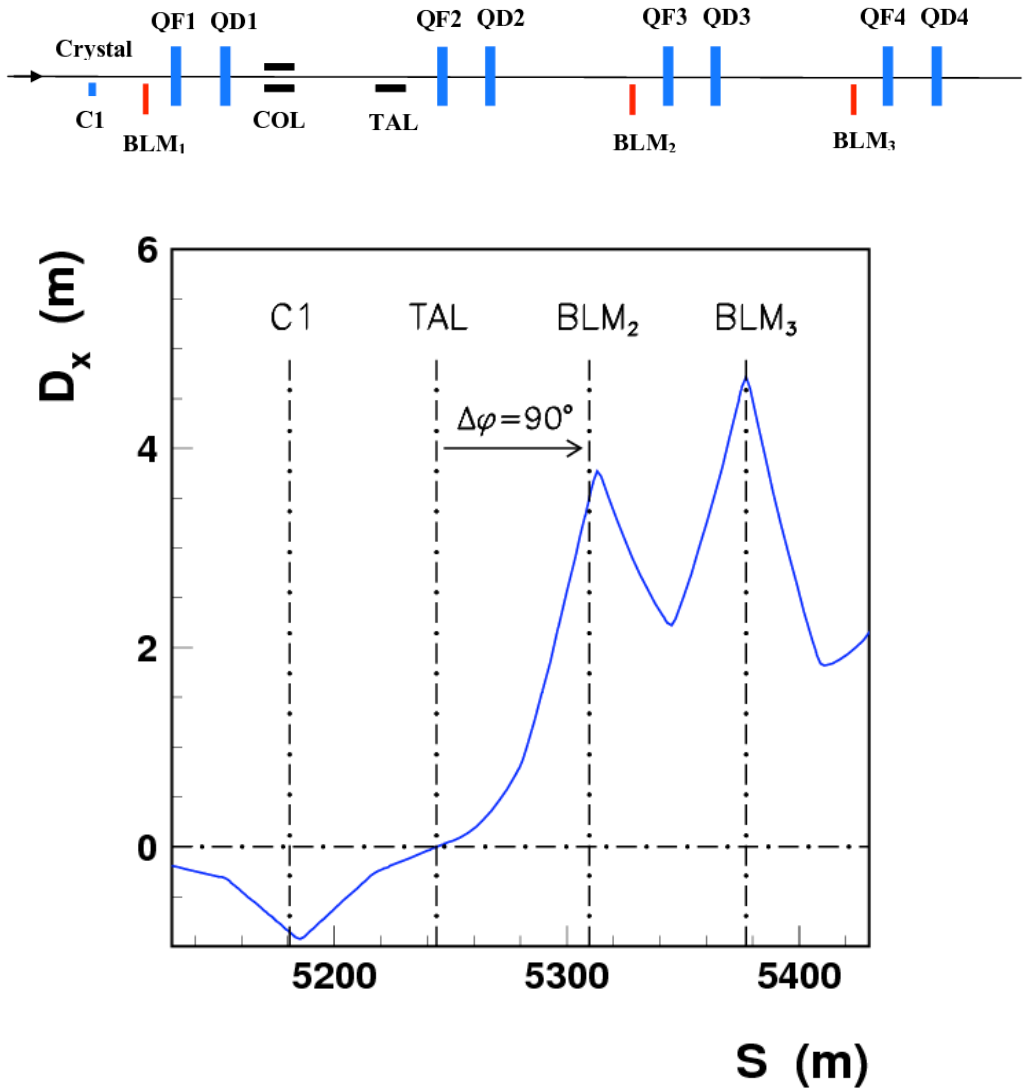

Fig. 8. The dependence of the dispersion function on the distance along the collimation area and the first HD area downstream of the absorber. Here C1, TAL, BLM_2 and BLM_3 are the positions of the crystal, the absorber, the beam loss monitors BLM_2 and BLM_3, respectively.

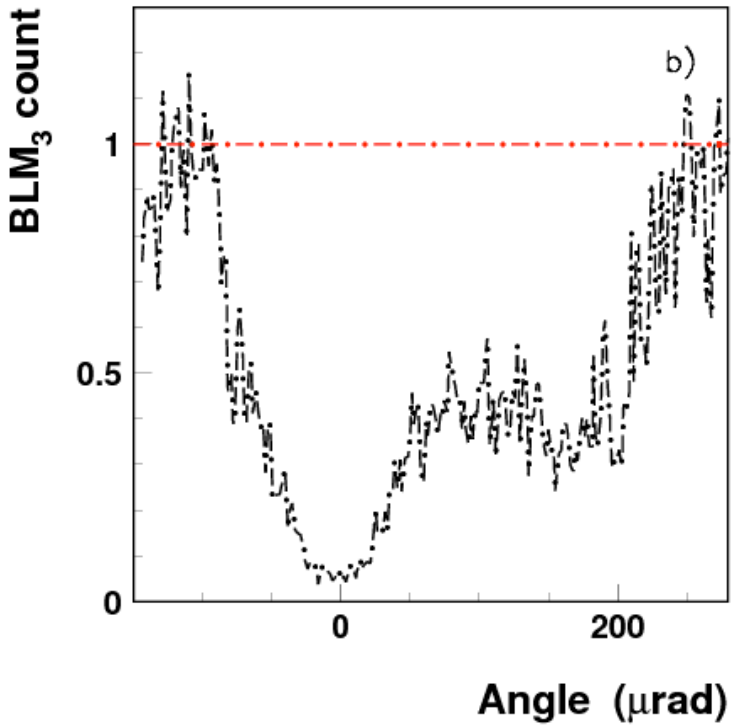

Fig. 9. The results of crystal assisted collimation of the SPS beam halo of 270 GeV/c protons. The dependence of beam losses observed in the HD area with the BLM_3 monitor on the angular position of the crystal normalized to its value for amorphous orientation of the crystal (dot-dashed line). The loss reduction in channeling condition is about 18.

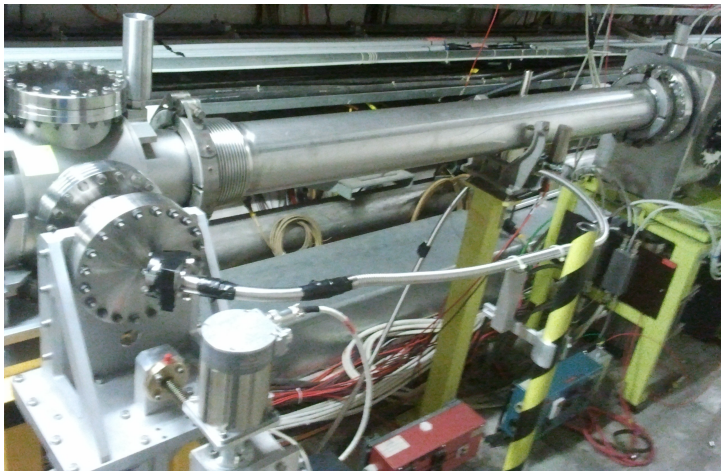

Fig. 10. The CpFM installed in the SPS tunnel.

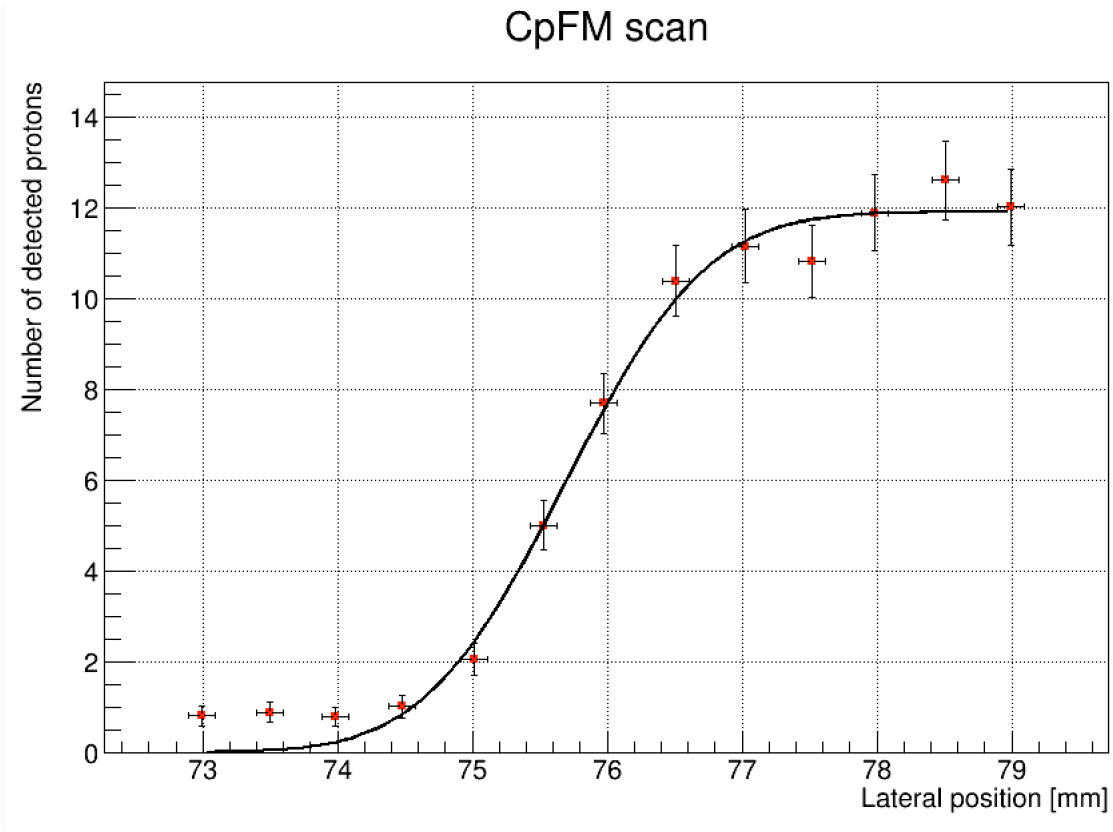

Fig. 11. Number of protons detected by the CpFM as a function of the radiator bar position in the vacuum pipe during crystal assisted collimation of the SPS beam halo of 270 GeV/c protons. The interpolating curve is an Err-function.

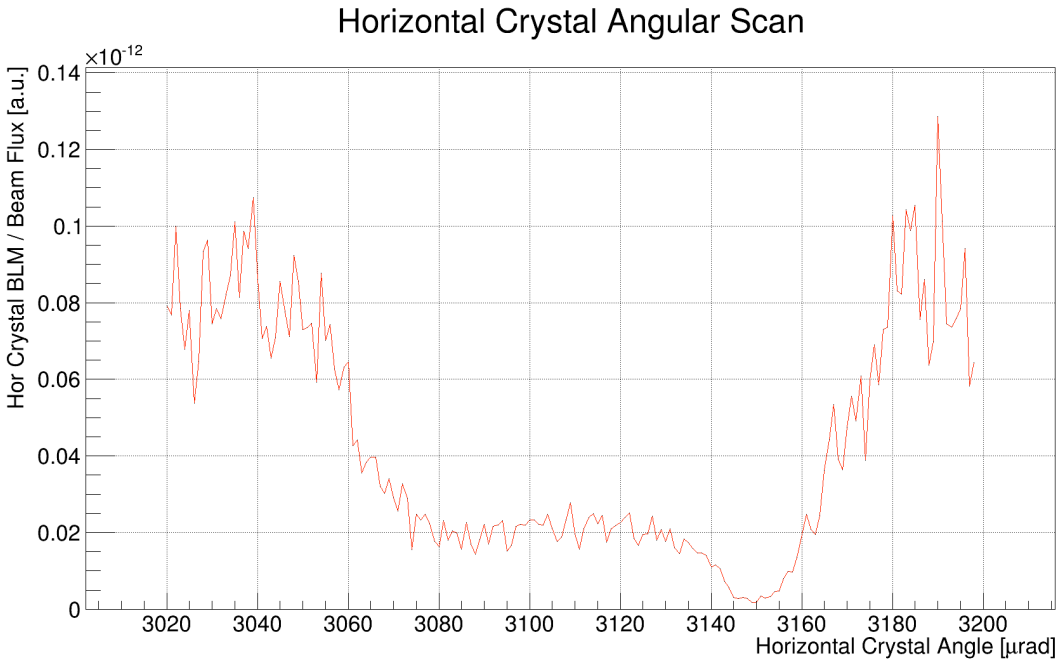

Fig. 12 – Horizontal crystal angular scan.

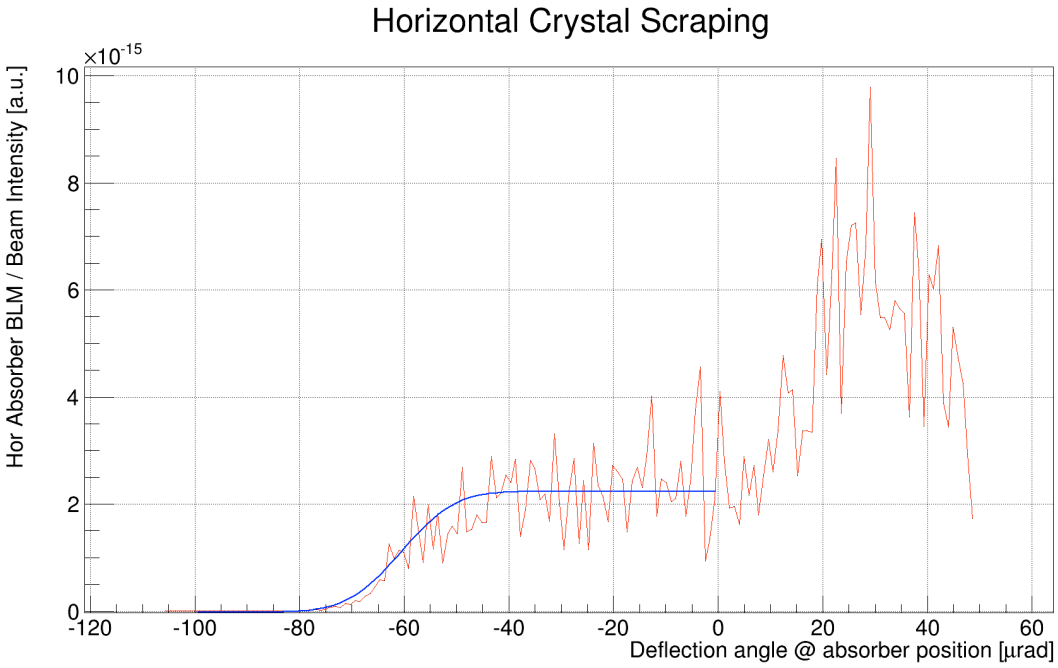

Fig. 13 – Horizontal crystal absorber scan. Crystal is fixed in channeling orientation. TCSG.B4L7 scrape the extracted beam.

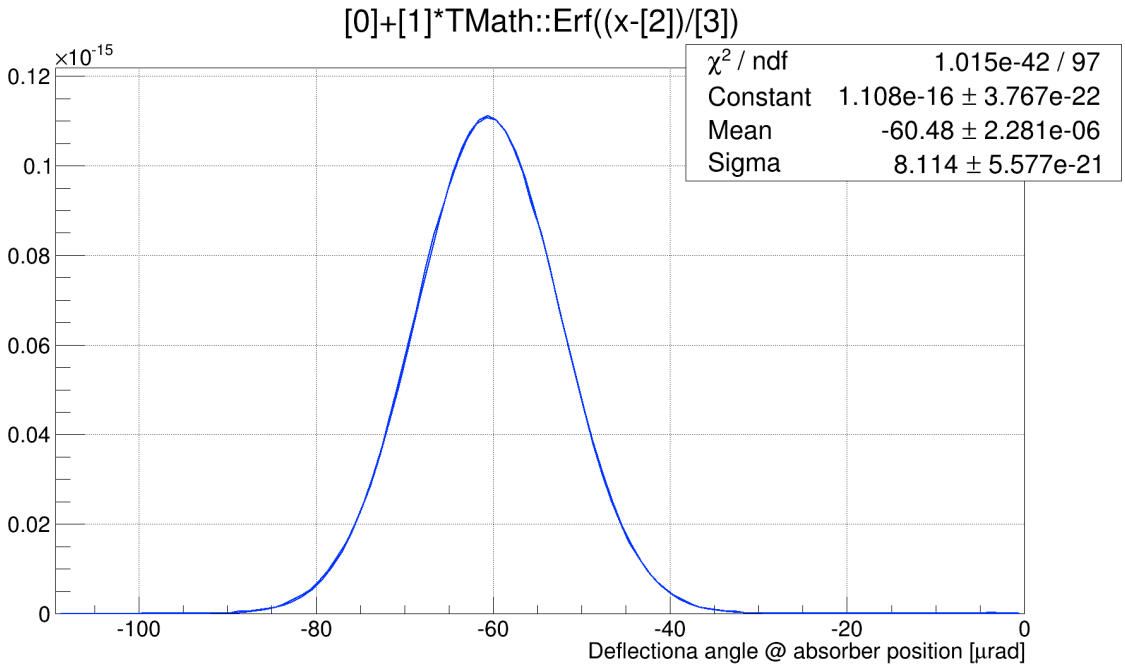

Fig.14 – Derivative of the error function, extracted beam profile. The mean value gives the deflection angle of the crystal.

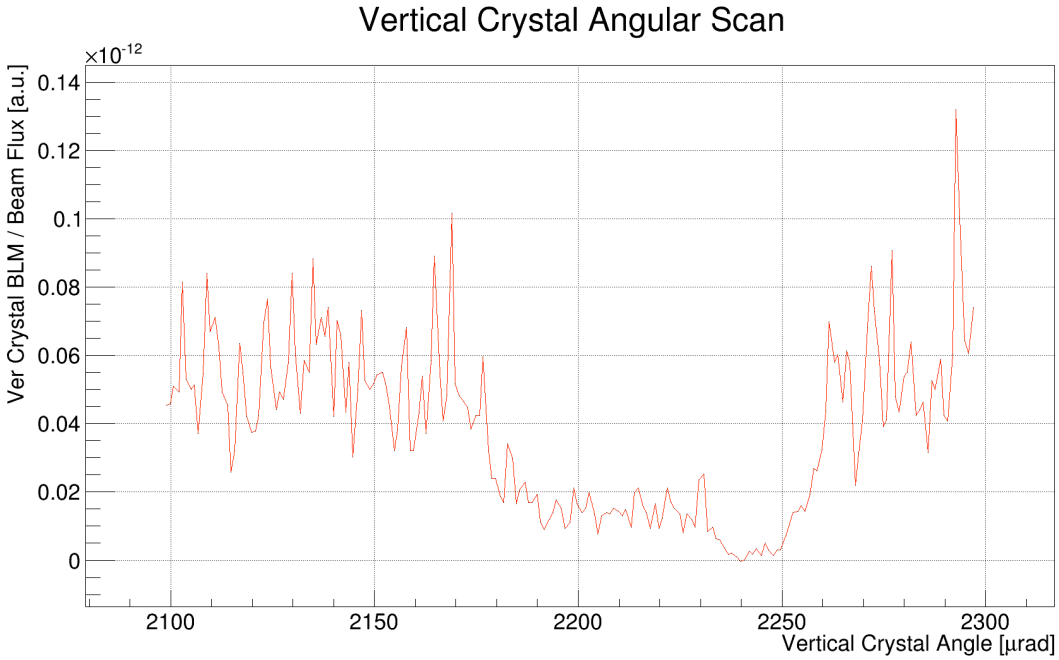

Fig. 15 – Vertical crystal angular scan.

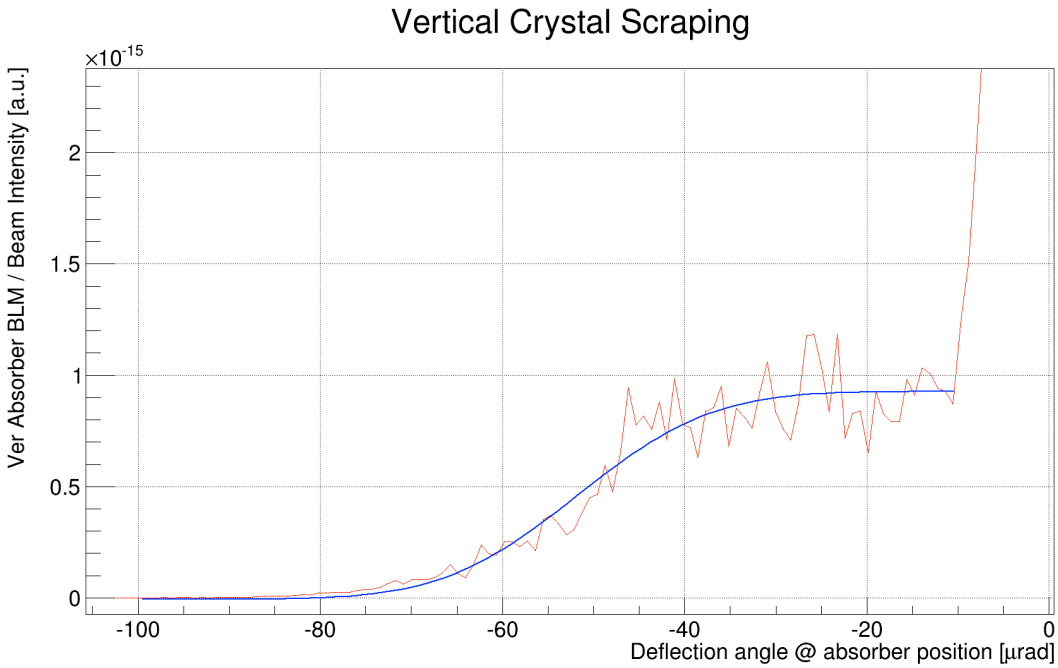

Fig. 16 – Vertical crystal absorber scan. Crystal is fixed in channeling orientation. TCSG.D4L7 scrape the extracted beam.

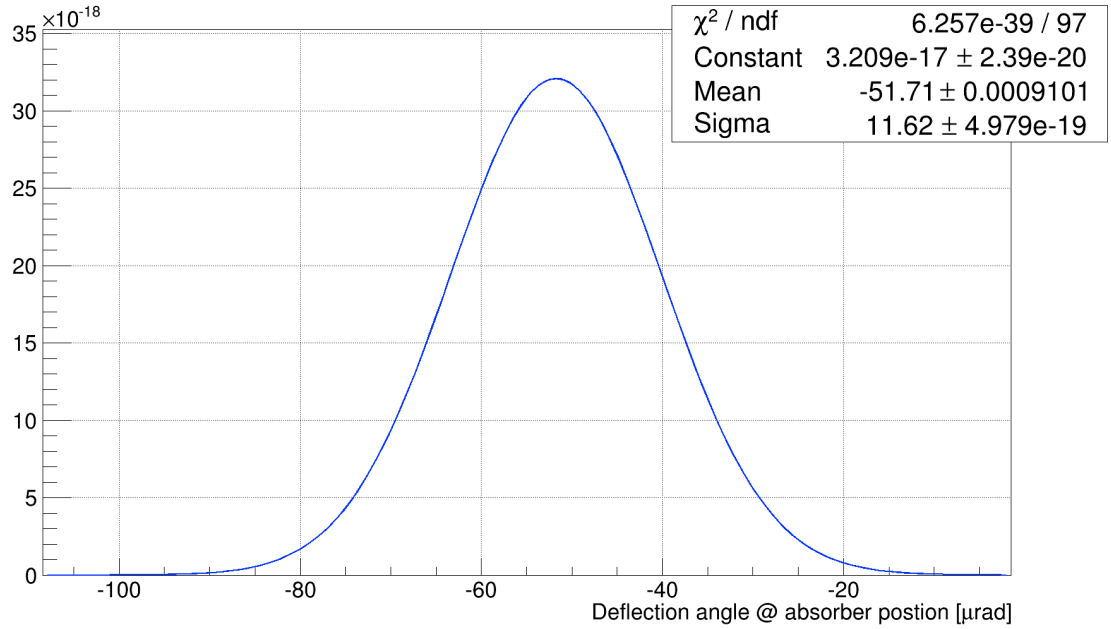

Fig. 17 – Derivative of the error function, extracted beam profile. The mean value gives the deflection angle of the crystal.